

BBA 72825

Ca²⁺-induced fusion of phosphatidylserine vesicles: mass action kinetic analysis of membrane lipid mixing and aqueous contents mixing

Jan Wilschut^a, Janny Scholma^a, Michal Bental^a,
Dick Hoekstra^a and Shlomo Nir^b

^a Laboratory of Physiological Chemistry, University of Groningen, Bloemsingel 10, 9712 KZ Groningen (The Netherlands)
and ^b The Seagram Centre for Soil and Water Sciences, Faculty of Agriculture, The Hebrew University of Jerusalem,
Rehovot 76100 (Israel)

(Received April 29th, 1985)

Key words: Membrane fusion; Phospholipid vesicle; Liposome; Phosphatidylserine; Ca²⁺

We have investigated the initial kinetics of Ca²⁺-induced aggregation and fusion of phosphatidylserine large unilamellar vesicles at 3, 5 and 10 mM Ca²⁺ and 15, 25 and 35°C, utilizing the Tb/dipicolinate (Tb/DPA) assay for mixing of aqueous vesicle contents and a resonance energy transfer (RET) assay for mixing of bilayer lipids. Separate rate constants for vesicle aggregation as well as deaggregation and for the fusion reaction itself were determined by analysis of the data in terms of a mass action kinetic model. At 15°C the aggregation rate constants for either assay are the same, indicating that at this temperature all vesicle aggregation events that result in lipid mixing lead to mixing of aqueous contents as well. By contrast, at 35°C the RET aggregation rate constants are higher than the Tb/DPA aggregation rate constants, indicating a significant frequency of reversible vesicle aggregation events that do result in mixing of bilayer lipids, but not in mixing of aqueous vesicle contents. In any conditions, the RET fusion rate constants are considerably higher than the Tb/DPA fusion rate constants, demonstrating the higher tendency of the vesicles, once aggregated, to mix lipids than to mix aqueous contents. This possibly reflects the formation of an intermediate fusion structure. With increasing Ca²⁺ concentrations the RET and the Tb/DPA fusion rate constants increase in parallel with the respective aggregation rate constants. This suggests that fusion susceptibility is conferred on the vesicles during the process of vesicle aggregation and not solely as a result of the interaction of Ca²⁺ with isolated vesicles. Aggregation of the vesicles in the presence of Mg²⁺ produces neither mixing of aqueous vesicle contents nor mixing of bilayer lipids.

Introduction

The search for plausible mechanisms of membrane fusion in biological systems has resulted in

extensive studies on fusion of negatively charged phospholipid vesicles induced by divalent cations [1,2]. Particularly, the Ca²⁺-induced aggregation and fusion of phosphatidylserine (PS) vesicles has been investigated in detail [3–22]. The development of the Tb/dipicolinate (Tb/DPA) assay enabled to demonstrate that the fusion reaction between PS vesicles takes place in the very initial stages of the aggregation process [6–8]. In addition, it could be demonstrated that mixing of aqueous vesicle contents precedes their release into

Abbreviations: DPA, dipicolinic acid; Hepes, 4-(2-hydroxyethyl)-1-piperazineethanesulfonic acid; LUV, large unilamellar vesicles; N-NBD-PE, N-(7-nitrobenz-2-oxa-1,3-diazol-4-yl)phosphatidylethanolamine; N-Rh-PE, N-(lissamine rhodamine B sulfonyl)phosphatidylethanolamine; PS, phosphatidylserine (bovine brain); RET, resonance energy transfer.

the external medium, indicating that the initial fusion events are largely non-leaky [6–8]. Mg^{2+} has been shown to produce aggregation of PS large unilamellar vesicles (LUV), but, in contrast to Ca^{2+} , it does not induce fusion or release of vesicle contents [9].

The data on Ca^{2+} -induced aggregation and fusion of PS vesicles obtained with the Tb/DPA assay have been analyzed in terms of a mass action kinetic model [10,14,15,19], which provides a means to determine separate rate constants for vesicle aggregation and for the fusion reaction itself. Following this approach, it has been shown that small unilamellar PS vesicles, due to their strong bilayer curvature, have a greater intrinsic fusion capacity than PS LUV [10,14].

In order to obtain more information about the mechanism of the fusion process in phospholipid vesicle systems, it is imperative to investigate the initial molecular events in the apposing lipid bilayers after vesicle aggregation, but before complete merging of the membranes and coalescence of the internal vesicle compartments is established. Recently, Struck et al. [23] have developed a fluorescent assay based on resonance energy transfer (RET) that allows continuous monitoring of the kinetics of membrane lipid mixing during vesicle fusion. Data obtained with this assay are also amenable to analysis in terms of the mass action kinetic model [24].

In the present paper we present a detailed comparison of the kinetics of membrane lipid mixing, based on results obtained with the RET assay, and aqueous contents mixing, based on results obtained with the Tb/DPA assay, during Ca^{2+} -induced aggregation and fusion of PS LUV. This comparison provides further insight into the molecular rearrangements occurring in the fusion reaction.

Materials and Methods

Materials. Bovine brain phosphatidylserine (PS), N-NBD-PE and N-Rh-PE were obtained from Avanti Polar Lipids, Inc. (Birmingham, AL). $\text{TbCl}_3 \cdot 6\text{H}_2\text{O}$ was from Aldrich (Brussels), dipicolinic acid (DPA) from Sigma Chemical Co. (St. Louis, MO). All other reagents were of the highest purity available.

Vesicle preparation. Large unilamellar vesicles (LUV) were prepared by reverse-phase evaporation and successive extrusion through 0.2 μm and 0.1 μm Unipore polycarbonate membranes (Bio-Rad, Richmond, CA), essentially as described before [7,25].

Vesicles to be used in the Tb/DPA assay were prepared in either one of the following aqueous media. (i) 5 mM TbCl_3 , 50 mM sodium citrate (Tb-vesicles), (ii) 50 mM sodium dipicolinate, 20 mM NaCl (DPA-vesicles) or (iii) 2.5 mM TbCl_3 , 25 mM sodium citrate, 25 mM sodium dipicolinate, 10 mM NaCl (Tb/DPA-vesicles). All the above media contained 5 mM Hepes, adjusted to a final pH of 7.4. Vesicles were separated from non-encapsulated material by gel filtration on Sephadex G-75 using 100 mM NaCl, 1.0 mM EDTA, 5 mM Hepes (pH 7.4) as elution buffer.

For the RET assay, 0.6 mol% each of N-NBD-PE and N-Rh-PE were incorporated in the vesicle bilayer. Vesicles were prepared in 100 mM NaCl, 0.1 mM EDTA, 5 mM Hepes (pH 7.4), as described above. Unlabeled vesicles were prepared in the same buffer.

Phospholipid phosphorus was determined according to the method of Böttcher et al. [26].

Fluorescence measurements. Mixing of aqueous vesicle contents was measured using the Tb/DPA assay, essentially as described previously [7–9,24]. A small aliquot (100 μl) of a concentrated 1:1 mixture of Tb- and DPA-vesicles was injected into a cuvette containing a final volume of 2.0 ml 100 mM NaCl, 0.1 mM EDTA, 5 mM Hepes (final concentrations) and CaCl_2 at the desired final concentration. The medium in the cuvette was stirred continuously and maintained at the desired temperature. Fluorescence was recorded continuously, using an SLM 8000 fluorimeter equipped with a double excitation monochromator (SLM/Aminco, Urbana, IL). Excitation and emission wavelengths were 276 and 545 nm, respectively, and a cut-off filter (< 530 nm) was placed between sample and emission monochromator [7]. The fluorescence scale was calibrated so that the 100% value corresponded to all of the Tb present being complexed to DPA [7].

Leakage of vesicle contents was measured by following the fluorescence quenching of pre-encapsulated Tb/DPA complex upon its release into

the external medium [15]. Measurements were carried out in the same way as the fusion measurements, except that one population of Tb/DPA-vesicles (at the same total phospholipid concentration as in the corresponding fusion measurements) was used. Calibration of the fluorescence scale was the same as in the corresponding fusion measurements and gave 100% initial fluorescence intensity in each of the release experiments.

The RET assay monitors continuously the relief of energy transfer between N-NBD-PE and N-Rh-PE, as the two probes dilute from a labeled into an unlabeled vesicle bilayer [23]. The increase of N-NBD-PE fluorescence was measured in a 1 : 1 mixture of labeled and unlabeled vesicles under conditions otherwise identical to those in the Tb/DPA assay. Excitation and emission wavelengths were 465 and 530 nm, respectively, with a cut-off filter (< 520 nm) between sample and emission monochromator. The fluorescence scale was calibrated so that the zero level corresponded to the initial residual fluorescence of the labeled vesicles and the 100% value to complete mixing of all the lipids in the system. The latter value was set by the fluorescence intensity of vesicles, labeled with 0.3 mol% each of the fluorophores, at the same total lipid concentration as that in the fusion assay. It should be noted that, in the concentration range of the fluorophores used, the N-NBD-PE fluorescence intensity increases linearly with the dilution of the probes [23,27].

Theoretical analysis

The fusion process is modeled to consist of two stages, the aggregation or close approach of the vesicles followed by the actual fusion reaction. Details of the theoretical analysis of vesicle fusion, monitored by the Tb/DPA assay, are given elsewhere [1,8,14,15]. Here we will just briefly describe the initial stages of the fusion process, where a fused doublet, denoted by F_2 , is formed from fusion of an aggregated dimer V_2 .



The rate of formation of V_2 from two single vesicles V_1 is of second order in the vesicle concentration,

and is described by the rate constant c_{11} ($M^{-1} \cdot s^{-1}$). The dimers V_2 can either fuse or deaggregate. These reactions are of first order with rate constants f_{11} (s^{-1}) and d_{11} (s^{-1}), respectively. If the inequality $f_{11} \gg c_{11}[V_0]$ holds, where $[V_0]$ is the initial molar concentration of the vesicles, then the aggregation is the rate-limiting step in the overall fusion process. Since the aggregation is of second order in the vesicle concentration (see Eqns. 2 to 4 below), it will be the rate-limiting step at low vesicle concentrations. At higher vesicle concentrations the fusion reaction itself will cause an increasingly significant delay.

The kinetic equations up to the doublet stage are

$$\frac{d[V_1]}{dt} = -2c_{11}[V_1]^2 + 2d_{11}[V_2] \quad (2)$$

$$\frac{d[V_2]}{dt} = c_{11}[V_1]^2 - f_{11}[V_2] - d_{11}[V_2] \quad (3)$$

$$\frac{d[F_2]}{dt} = f_{11}[V_2] \quad (4)$$

These equations can be solved by numerical integration, as described recently in detail for the case of fusion between virus particles and phospholipid vesicles [28]. The procedure can also be applied to the analysis of fusion among phospholipid vesicles monitored with the Tb/DPA or RET assay, as it explicitly distinguishes between two species of particles, e.g. the Tb- and DPA-vesicles in the Tb/DPA assay or the labeled and unlabeled vesicles in the RET assay. This is done by presenting V_1 , V_2 and F_2 as vector quantities. For example, in the Tb/DPA assay, $V(1,0)$ and $V(0,1)$ denote a Tb- and a DPA-vesicle, respectively, and $V(2,0)$, $V(1,1)$ and $V(0,2)$ denote a dimer consisting of two Tb-vesicles, one Tb- and one DPA-vesicle, and two DPA-vesicles, respectively. Similarly, a fused doublet is represented by $F(2,0)$, $F(1,1)$ or $F(0,2)$.

In the first round of fusion in a 1 : 1 mixture of the two different vesicle species, only 50% of the fusion events, i.e. the formation of $F(1,1)$ but not of $F(2,0)$ or $F(0,2)$, is productive in terms of fluorescence development. In the Tb/DPA assay, the fluorescence scale is calibrated so that this would result in maximally 50% fluorescence in-

crease [7,8]. In the RET assay, the initial probe concentrations (0.6 mol% each) are such that the N-NBD-PE fluorescence intensity increases linearly with the dilution of the probes [23,27]. The fluorescence scale is calibrated to 100% for the hypothetical situation in which all the vesicles have fused to a completely mixed membrane system. Therefore in the RET assay the first round of fusion in a 1 : 1 mixture of labeled and unlabeled vesicles produces, as in the Tb/DPA assay, also a maximum of 50% fluorescence increase. At later stages, i.e. when fusion products include more particles, the fluorescence increase in the RET assay is somewhat smaller than that in the Tb/DPA assay, but initially (up to a fluorescence increase of 30–40%) the relative difference is marginal. Nevertheless, in the analysis the difference is taken into account.

The current procedure of numerical calculation considers aggregation-fusion products including up to 16 particles and is applicable to systems containing any ratio of the fusing species.

In practice the analysis is carried out as follows. First, the aggregation rate constant, c_{11} , is determined from the results at a low vesicle concentration, where aggregation is rate-limiting to the overall fusion process, i.e. $f_{11} \gg c_{11}[V_0]$. Then the fusion rate constant, f_{11} , is determined from the results obtained with a concentrated vesicle suspension. The results at other vesicle concentrations provide a test of the predictions and a fine tuning of the values of the parameters.

In the first stages of the analysis, we employ a simple analytical expression, rather than the more exact numerical integration, to calculate the increase of fluorescence with time. This analytical solution has been shown [14] to yield a very good approximation to the more exact solutions, up to fluorescence levels of about 20%. The approximate expression for $F(t)$ is

$$F(t) = 100A(t)\mathcal{F}(t) \quad (5)$$

where

$$A(t) = (1 + 4\hat{c}_{11}[V_0]t)^{1/4} - 1$$

$$\mathcal{F}(t) = 1 + \frac{\exp(-\hat{f}_{11}t) - 1}{\hat{f}_{11}t}$$

and

$$\hat{c}_{11} = c_{11}/(1 + d_{11}/f_{11}) \quad (6)$$

$$\hat{f}_{11} = f_{11} + d_{11} \quad (7)$$

The quantities \hat{c}_{11} and \hat{f}_{11} (the apparent, effective values of c_{11} and f_{11} , respectively) are equal to c_{11} and f_{11} , respectively, when d_{11} equals 0. As shown before [14], the initial stages of the fusion process (up to $F(t) = 20\%$) can be simulated by several sets of c_{11} , f_{11} and d_{11} . Hence, having determined \hat{c}_{11} and \hat{f}_{11} by the application of Eqn. 5, we employ the exact numerical calculations, up to $F(t) = 40\%$, to determine the set of c_{11} , f_{11} and d_{11} which gives the best fit to the experimental data.

Results

Lipid mixing vs. aqueous contents mixing

Fig. 1 shows a comparison between results obtained with the Tb/DPA assay and the RET assay during fusion of PS LUV at 5 mM Ca^{2+} and 25°C. In the Tb/DPA assay a 1 : 1 mixture of Tb- and DPA-vesicles was injected into a medium containing 5 mM Ca^{2+} and the increase of the Tb fluorescence was recorded continuously (curve a). In the RET assay the increase of N-NBD-PE fluorescence was measured, using a 1 : 1 mixture of labeled and unlabeled vesicles, under otherwise identical conditions (curve d). The fluorescence intensity in the Tb/DPA assay is affected by the release of vesicle contents, due to dissociation of the Tb/DPA complex in the external EDTA-containing medium [6,7]. This is illustrated by the secondary decrease of the fluorescence in curve a. In a parallel experiment the kinetics of dissociation of the Tb/DPA complex were determined directly (curve b). Here one population of vesicles containing the Tb/DPA complex was used and the decrease of the fluorescence intensity was followed under conditions otherwise identical to those in the fusion assay. In agreement with previous observations [6–9,16], the mixing of vesicle contents clearly preceded their release, indicating that initially the fusion process is essentially non-leaky. Curve c in Fig. 1 presents the corrected kinetics of mixing of aqueous contents, i.e. the fluorescence that would be obtained in the fusion assay if no

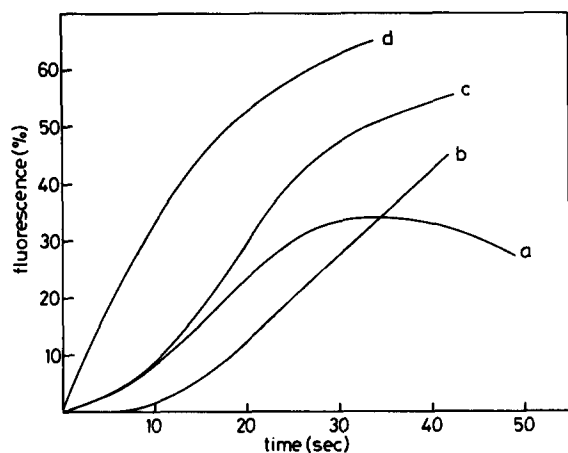


Fig. 1. Fluorescence development during Ca^{2+} -induced fusion of PS LUV at 25°C , monitored with the Tb/DPA assay or the RET assay. Curve a, a 1:1 mixture of Tb- and DPA-vesicles was injected into a medium containing 5 mM CaCl_2 (final concentration); final PS concentration was $50 \mu\text{M}$. The increase of the Tb fluorescence intensity was monitored continuously. Curve b, Tb/DPA-vesicles were injected into the Ca^{2+} -containing medium to the same final PS concentration as in (a) and the decrease of the fluorescence intensity was monitored continuously. Curve c, corrected Tb fluorescence intensity, obtained by addition of half of curve b to curve a. Curve d, a 1:1 mixture of vesicles labeled with N-NBD-PE and N-Rh-PE and unlabeled vesicles was injected into the Ca^{2+} -containing medium under conditions otherwise identical to those in (a) and the increase of the N-NBD-PE fluorescence intensity was recorded.

leakage was occurring. Curve c was calculated by adding half of the dissociation values (curve b) to the Tb fluorescence observed in the fusion assay (curve a). The factor 0.5 arises from the fact that in the initial stages of the process only 50% of the fusion events in a 1:1 mixture of Tb- and DPA-vesicles is productive in terms of fluorescence development [7,8]

As outlined above, the calibration of the fluorescence scales in the Tb/DPA and RET assays was such that the initial kinetics can be compared directly. Clearly, mixing of bilayer lipids (Fig. 1, curve d) was considerably faster than the mixing of aqueous vesicle contents, even after correction of the latter for release (Fig. 1, curve c).

Mass action kinetic analysis

To determine the separate rate constants for vesicle aggregation and for the fusion reaction

itself, \hat{c}_{11} and \hat{f}_{11} , measurements were carried out at different vesicle concentrations, utilizing both the Tb/DPA and the RET assay at 5 mM Ca^{2+} and 25°C . For each condition duplicate measurements were done and their results agreed to within 1–2% fluorescence. The data were fitted to the model, utilizing the approximation for the development of fluorescence with time, presented in Eqn. 5. The data points in Fig. 2A represent the percentage Tb fluorescence, corrected for release of vesicle contents, while the drawn lines represent

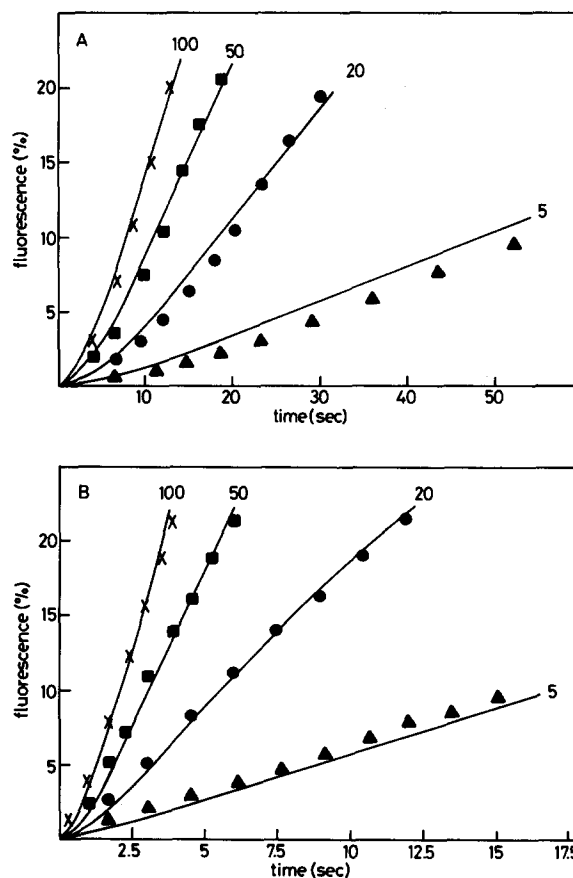


Fig. 2. Mass action kinetic simulation of Ca^{2+} -induced fusion of PS LUV at 25°C , monitored with the Tb/DPA assay (A) or the RET assay (B). Fusion was measured at 5 mM Ca^{2+} at different vesicle concentrations. Total micromolar PS concentrations are indicated. The data points represent experimental fluorescence intensities (in the case of the Tb/DPA assay corrected for leakage of vesicle contents) and the drawn lines the theoretical simulation, according to the approximation presented in Eqn. 5, that gave an optimal fit to the data. Note the difference in time scale between (A) and (B).

the theoretical simulation. An optimal fit to the data was obtained with $\hat{c}_{11} = 5.5 \cdot 10^7 \text{ M}^{-1} \cdot \text{s}^{-1}$ and $\hat{f}_{11} = 0.1 \text{ s}^{-1}$.

Fig. 2B presents the corresponding results obtained with the RET assay. In this case the experimental data could be best simulated by employing the rate constants: $\hat{c}_{11} = 1.3 \cdot 10^8 \text{ M}^{-1} \cdot \text{s}^{-1}$ and $\hat{f}_{11} = 0.6 \text{ s}^{-1}$.

Effects of Ca^{2+} concentration and temperature

The overall rate of Ca^{2+} -induced fusion of PS LUV has been shown to be strongly dependent on both Ca^{2+} concentration and temperature [7,12, 20–22]. Therefore, we now compared the kinetics of lipid mixing with the kinetics of aqueous contents mixing at three Ca^{2+} concentrations (3, 5 and 10 mM), each at three temperatures (15, 25 and 35°C). For each condition duplicate measurements were done at four different vesicle concentrations and the results were fitted to the kinetic model as described above, providing separate rate constants for the aggregation and for the fusion reaction per se. For fitting of the data we primarily employed the analytical approximation in Eqn. 5. In several cases numerical integration was employed as well. For the initial stages of the process the results of

either approach were the same. For the sake of brevity, the fit to the data for all of the conditions is not shown. A survey of the rate constants is given in Table I.

The results in Table I show that at 15°C the aggregation rate constants for the Tb/DPA assay were the same as the corresponding values for the RET assay. In contrast, at 35°C the aggregation rate constants obtained with the RET assay were, depending on the Ca^{2+} concentration, 4–7-fold higher than the corresponding values for the Tb/DPA assay. Under all conditions the fusion rate constants obtained with the RET assay were higher than the corresponding fusion parameters for the Tb/DPA assay. This is clearly illustrated in Fig. 3 by the fluorescence curves observed at high lipid concentrations, where the fusion reaction itself determines the rate of the overall process to a considerable extent.

Another aspect of the results in Table I is presented in Fig. 4, where the values of the rate constants are plotted as a function of the Ca^{2+} concentration. At each of the temperatures studied, the fusion rate constants obtained with either assay increased with increasing Ca^{2+} concentration remarkably in parallel with the corresponding aggregation rate constants.

TABLE I

Ca^{2+} -INDUCED AGGREGATION AND FUSION OF PS LUV: SURVEY OF RATE CONSTANTS

Fusion was measured (as described in the legends to Figs. 1 and 2) at 15, 25 and 35°C, at 3, 5 and 10 mM Ca^{2+} , and at 5, 20, 50 and 100 μM PS. The results were analyzed in terms of the mass action kinetic model utilizing the approximation in Eqn. 5. Values of the parameters presented are apparent values, not corrected for a possible effect of reversibility of aggregation. The estimated relative uncertainty of the values is approx. ± 30 –50%, depending on the fit of the data at each particular condition.

t (°C)	$[\text{Ca}^{2+}]$ (mM)	Aggregation rate constant, $\hat{c}_{11} (\text{M}^{-1} \cdot \text{s}^{-1}) (\times 10^{-7})$		Fusion rate constant, $\hat{f}_{11} (\text{s}^{-1})$	
		Tb/DPA	RET	Tb/DPA	RET
15	3	1.3	1.0	0.006	0.03
	5	3.9	3.5	0.012	0.12
	10	7.6	4.2	0.022	0.18
25	3	1.7	3.3	0.03	0.17
	5	5.5	13	0.1	0.6
	10	8.0	25	0.2	1.5
35	3	2.2	8.0	0.12	$\geq 1^a$
	5	8.0	34	0.3	$\geq 5^a$
	10	12	85	0.55	$\geq 10^a$

^a These values are lower bounds; at higher values of f_{11} the ratio $f_{11}/c_{11} [V_o]$ (see Theoretical section) becomes such that even at 100 μM PS the process is essentially rate-limited by the aggregation step, implying that f_{11} cannot be estimated reliably anymore (see also Ref. 22).

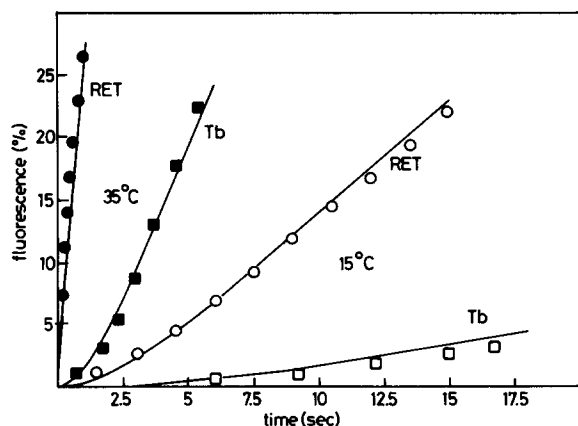


Fig. 3. Mass action kinetic simulation of PS LUV fusion at 15°C (open symbols) and 35°C (closed symbols), monitored with the Tb/DPA assay (squares) or the RET assay (circles). Fusion was measured at 5 mM Ca^{2+} at different vesicle concentrations. For clarity only the results at 100 μM PS are shown. The data points represent the experimental fluorescence intensities and the drawn lines the theoretical simulation, obtained with the approximation shown in Eqn. 5.

Effect of deaggregation of vesicle aggregates

In the analysis of the fusion data presented above, we primarily employed the analytical approximation in Eqn. 5, which does not explicitly take into account the possibility that deaggregation of aggregated vesicles may occur. Therefore,

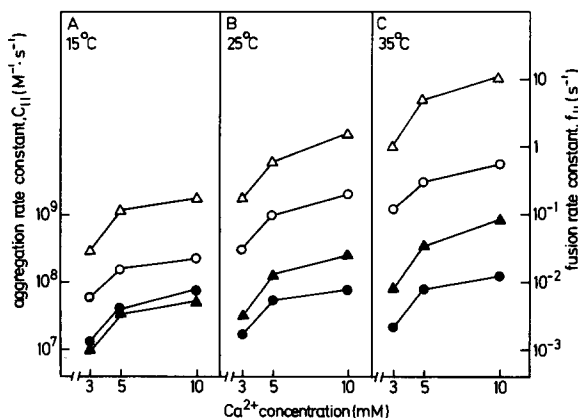


Fig. 4. Dependence of the aggregation and fusion rate constants for PS LUV interaction on the Ca^{2+} concentration at 15°C (A), 25°C (B) and 35°C (C). Circles, parameters for the Tb/DPA assay; triangles, parameters for the RET assay. Filled symbols, aggregation rate constants; open symbols, fusion rate constants.

the constants in Table I represent apparent, effective parameters, denoted in the theoretical section by \hat{c}_{11} and \hat{f}_{11} . Ignoring reversibility of vesicle aggregation may not be justified, but, as outlined in the theoretical section and in Refs. 14 and 15, neither the approximation (Eqn. 5), which is valid only up to fluorescence levels of about 20%, nor numerical integration up to the same fluorescence levels allow discrimination between several different combinations of c_{11} , f_{11} and d_{11} . This implies that the apparent values of the rate constants in Table I may deviate from their true values, as shown in Eqns. 6 and 7.

To assess the extent to which vesicle deaggregation affects the rate constants presented in Table I, we performed experiments utilizing the Tb/DPA assay at different concentrations of a 1:1 mixture of Tb- and DPA-vesicles, and the corresponding numerical integrations up to fluorescence levels of 40%. The data at 25°C could be simulated only by setting the ratio d_{11}/f_{11} close to zero, as shown in Fig. 5A. The conclusion that d_{11}/f_{11} is close to zero does not necessarily mean that d_{11} equals zero, but rather that $d_{11} \ll f_{11}$, which amounts to saying that the vesicles do not get the chance to deaggregate, since they fuse much faster. At 35°C (Fig. 5B) the data could be best simulated by setting the ratio d_{11}/f_{11} to 0.5 or 1.0.

The above results imply that for the Tb/DPA assay the aggregation and fusion parameters at the lower temperatures, as presented in Table I, are essentially equal to their true values. At 35°C the true aggregation rate constants are about 2-fold higher (see Eqn. 6), while the true fusion rate constants are about half of the apparent values (see Eqn. 7). A similar evaluation of the effect of reversibility of vesicle aggregation in the case of the RET assay was not feasible, since, as discussed more extensively below, lipid mixing occurs during reversible vesicle-vesicle interactions.

Effects of Mg^{2+}

It has been demonstrated previously that Mg^{2+} induces massive aggregation of PS LUV, but no mixing or release of aqueous vesicle contents [9]. We confirmed this observation in the present study: no fluorescence increase was detected with the Tb/DPA assay at 10 mM Mg^{2+} and either 15, 25 or 35°C (not shown). Essentially the same

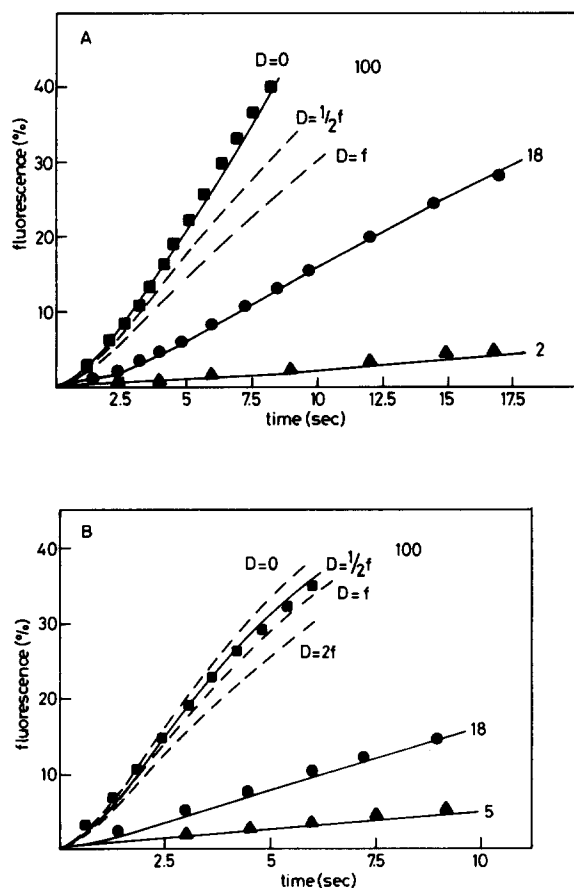


Fig. 5. Reversibility of PS LUV aggregation in the presence of 5 mM Ca^{2+} at 25°C (A) and 35°C (B). Fusion was measured with the Tb/DPA assay, with a 1:1 mixture of Tb- and DPA vesicles, at different vesicle concentrations. Total micromolar PS concentrations are indicated. The data points represent the experimental fluorescence intensities. Calculations were carried out utilizing the procedure of numerical integration. In (A) the drawn lines were obtained by setting d_{11} equal to zero. In (B) the drawn lines represent the simulation obtained by setting $d_{11} = 1/2f_{11}$. The dashed lines give the simulations at 100 μM PS for other values of d_{11} . The rate constants obtained were higher than the corresponding values in Table I, since in this particular experiment the PS LUV preparation was centrifuged to remove the larger vesicles (see Ref. 22). At 25°C, $c_{11} = 1.4 \cdot 10^8 \text{ M}^{-1} \cdot \text{s}^{-1}$, $d_{11} = 0 \text{ s}^{-1}$ and $f_{11} = 0.25 \text{ s}^{-1}$; at 35°C, $c_{11} = 1.4 \cdot 10^8 \text{ M}^{-1} \cdot \text{s}^{-1}$, $d_{11} = 0.4 \text{ s}^{-1}$ and $f_{11} = 0.8 \text{ s}^{-1}$.

results were obtained with the RET assay (not shown), indicating that aggregation of PS LUV in the presence of Mg^{2+} does not produce mixing of bilayer lipids.

Discussion

In this study the kinetics of bilayer lipid mixing and aqueous vesicle contents mixing during Ca^{2+} -induced fusion of PS LUV have been investigated. In agreement with previous observations by Ababei and Hildenbrand [18], the results show that in this system under all conditions examined the overall rate of lipid mixing is considerably faster than that of aqueous vesicle contents mixing.

Coalescence of internal vesicle volumes obviously requires fusion of the vesicles. Mixing of bilayer lipids, on the other hand, may also occur through other, non-fusion processes, such as transfer or exchange of individual lipid molecules through the aqueous medium or during transient collisions between the vesicles. The mass action kinetic analysis, presented here, allows discrimination between these possible mechanisms of lipid mixing. The kinetic model views the overall process of vesicle interaction as consisting of a second-order step of vesicle aggregation followed by the first-order fusion reaction itself. The data obtained with the RET assay could be well simulated by this model, indicating that lipid mixing is dependent on vesicle-vesicle interaction. This rules out the possibility of transfer or exchange of individual lipid molecules through the aqueous medium, consistent with earlier observations on the non-exchangeability of N-NBD-PE and N-Rh-PE [12,23,29,30].

The rate constants in Table I clearly demonstrate that the faster rate of lipid mixing, as compared to that of aqueous contents mixing, arises primarily at the level of the fusion reaction itself. Under all conditions studied the fusion parameters for the RET assay are considerably higher than the corresponding fusion parameters for the Tb/DPA assay, indicating that the vesicles, after aggregation, have a greater tendency to mix their lipids than to mix their internal contents. This could be due to rapid transfer or exchange of individual lipid molecules between aggregated vesicles. However, the absence of lipid mixing after aggregation of the vesicles in the presence of Mg^{2+} indicates that aggregation in itself is not a sufficient condition for mixing of lipids to occur. It is well-established that aggregates of PS bilayers in the presence of Mg^{2+} are hydrated, leaving a layer of

water between the apposing membranes [5]. By contrast, Ca^{2+} causes complete dehydration of the apposing bilayer surfaces, thus establishing direct inter-membrane contact [5]. This capacity of Ca^{2+} has been proposed to be of critical importance in the induction of PS vesicle fusion [5,9,12,21,31]. Since the relatively fast lipid mixing between aggregated PS vesicles occurs only in the presence of Ca^{2+} , and not with Mg^{2+} , it appears that this lipid mixing process is directly related to the fusion reaction. We propose that it is the first step in the destabilization of the vesicle bilayers and that it may represent the formation of a fusion intermediate in which the outer lipid monolayers of the fusing vesicles already form a continuous structure, while the inner monolayers and the internal compartments are still separate (Fig. 6B).

Our present results may seem to be in disagreement with results of previous studies on bilayer lipid and aqueous contents mixing during fusion of PS SUV [13,16] or cardiolipin-containing LUV [24], which showed essentially no difference between the relative kinetics of the two processes at

25°C. It should be noted, however, that in these systems the rate of the coalescence of internal vesicle volumes (f_{11} obtained with the Tb/DPA assay) is much higher than the rate obtained here for PS LUV under conditions of comparable rates of aggregation. This implies that, at least at 25°C, the fast lipid mixing as a prelude to the total merging of the bilayers may not be distinguishable in these systems. Interestingly, with cardiolipin-containing LUV at 37°C, rather than 25°C, the fusion rate constants obtained with the RET assay are significantly higher than the corresponding fusion parameters for the Tb/DPA assay [24], in agreement with the results presented here. This suggests that there is no essential difference between cardiolipin-containing LUV and PS LUV in this respect, except in that the PS LUV appear to remain relatively long in an intermediary fusion stage before complete merging of the bilayers is established.

The results in Table I show that at 15°C the corresponding aggregation rate constants for the RET and the Tb/DPA assay are the same. This indicates that at this temperature all vesicle aggregation events that produce mixing of bilayer lipids result in mixing of aqueous contents as well. At 25 and 35°C the aggregation rate constants for the RET assay are higher than the corresponding values for the Tb/DPA assay. In view of the limits of accuracy of the parameters, at 25°C the difference between the respective constants is marginal. However, at 35°C the values for the RET assay are significantly (on the average about 5-fold) higher than those for the Tb/DPA assay. It is unlikely that this discrepancy is due to differences between the vesicles used in the RET assay and those used in the Tb/DPA assay, since in that case one would have expected deviating results at 15°C as well, which were not observed. Rather, we believe that the relatively high aggregation rate constants for the RET assay indicate that, particularly at higher temperatures, the frequency of vesicle aggregation events that produce lipid mixing is higher than the frequency of aggregation events that eventually lead to mixing of aqueous vesicle contents. This conclusion has an intriguing implication, as it indicates that reversible aggregation events occur that do result in mixing of bilayer lipids, but not in mixing of aqueous vesicle con-

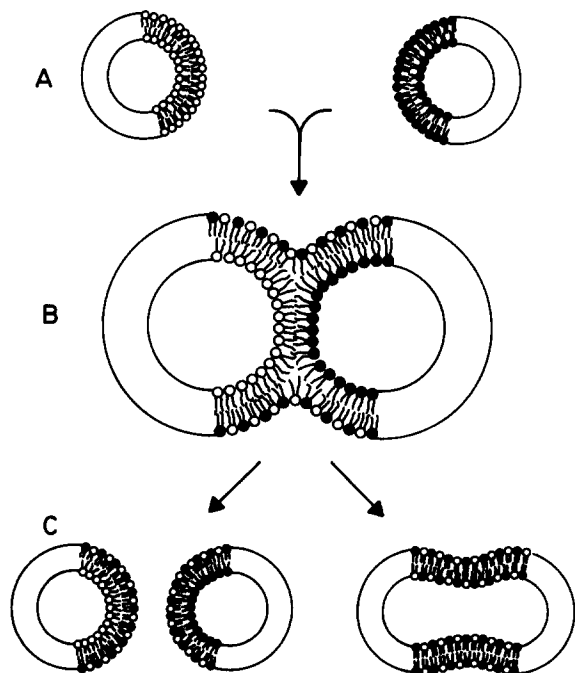


Fig. 6. Hypothetical mechanism of Ca^{2+} -induced PS LUV interaction.

tents. As argued above, lipid mixing is likely to be related to the formation of fusion intermediates. Therefore, the occurrence of reversible vesicle aggregation events that produce mixing of bilayer lipids suggests that the formation of a fusion intermediate does not necessarily result in the irreversible formation of a fusion product (Fig. 6C). A direct consequence of this result is that relying on a lipid mixing assay as the only measure for membrane fusion may not always be justified and that the results obtained with lipid mixing assays should be interpreted with caution.

The above conclusion that, particularly at higher temperatures, the aggregation of PS LUV in the presence of Ca^{2+} is partly reversible is supported by the analysis of deaggregation rates presented in Fig. 5. The results obtained with the Tb/DPA assay at 35°C could only be simulated by assuming a d_{11}/f_{11} ratio of 0.5–1.0. As a consequence, the true forward aggregation rate constants at this temperature are approx. 2-fold higher than the apparent values presented in Table I (see Eqn. 6). These true aggregation rate constants approach to within the limits of accuracy the corresponding rate constants for the RET assay, implying that, indeed, the reversible aggregation events that do not result in mixing of aqueous vesicle contents, do result in mixing of bilayer lipids.

As expected, the rate constants for PS vesicle aggregation increase with increasing Ca^{2+} concentrations (Table I, Fig. 4), due to enhanced Ca^{2+} binding to the vesicles. More remarkable is the observation that the fusion rate constants increase in parallel with the aggregation rate constants. This apparent correlation between the two parameters suggests that the tendency of the vesicles to fuse after aggregation is determined by their tendency to aggregate. In a previous study we have observed a similar correlation between aggregation and fusion for cardiolipin-containing LUV [24]. As an explanation, we have proposed that the structural changes in the vesicle bilayer that render the vesicles susceptible to fusion are induced by vesicle-vesicle contact rather than solely by interaction of Ca^{2+} with dispersed vesicles in the stage before aggregation. By analogy, we suggest a similar mechanism for the Ca^{2+} -induced interaction between PS vesicles (see also Ref. 21). It should be emphasized, however, that it is not the aggregation

per se that confers fusion susceptibility to the vesicles, as is clear from the effect of Mg^{2+} on PS LUV (Ref. 9, and this paper). Rather, in systems where fusion does occur, the potential fusion capacity appears to materialize into a significant bilayer destabilization only during vesicle-vesicle interaction. The idea of a contact-induced vesicle destabilization is in agreement with suggestions of Rand and Parsegian [32]. However, these authors tend to conclude that membrane-membrane contact induces a complete rupture of the vesicles. In contrast, we propose that after aggregation the vesicles fuse initially. This conclusion is based on extensive data showing that in the initial stages of interaction between phospholipid vesicles a largely non-leaky coalescence of internal compartments is established [6–10,14–16,20–22,24]. The rupture of the fusion products appears to be a secondary process, most likely due to the lack of internal control in these systems. Thus, eventually very large aggregation and fusion products are formed that are unlikely to remain in a closed vesicular configuration.

Acknowledgements

We thank Mrs. Rinske Kuperus for excellent secretarial assistance, and Dr. Gerrit Scherphof for his encouragement and interest in the project. This work was supported by the European Molecular Biology Organization (short-term fellowship to S.N.).

References

- 1 Nir, S., Bentz, J., Wilschut, J. and Düzgüneş, N. (1983) *Prog. Surf. Sci.* 13, 1–124
- 2 Wilschut, J. and Hoekstra, D. (1984) *Trends Biochem. Sci.* 9, 479–483
- 3 Papahadjopoulos, D., Vail, W.J., Newton, C., Nir, S., Jacobson, K., Poste, G. and Lazo, R. (1977) *Biochim. Biophys. Acta* 465, 579–598
- 4 Papahadjopoulos, D., Vail, W.J., Jacobson, K. and Poste, G. (1975) *Biochim. Biophys. Acta* 394, 483–491
- 5 Portis, A., Newton, C., Pangborn, W. and Papahadjopoulos, D. (1979) *Biochemistry* 18, 780–790.
- 6 Wilschut, J. and Papahadjopoulos, D. (1979) *Nature* 281, 690–692
- 7 Wilschut, J., Düzgüneş, N., Fraley, R. and Papahadjopoulos, D. (1980) *Biochemistry* 19, 6011–6021
- 8 Nir, S., Bentz, J. and Wilschut, J. (1980) *Biochemistry* 19, 6030–6036

- 9 Wilschut, J., Düzgüneş, N. and Papahadjopoulos, D. (1981) *Biochemistry* 20, 3126–3133.
- 10 Nir, S., Wilschut, J. and Bentz, J. (1982) *Biochim. Biophys. Acta* 688, 275–278
- 11 Miller, D.C. and Dahl, G.P. (1982) *Biochim. Biophys. Acta* 689, 165–169
- 12 Hoekstra, D. (1982) *Biochemistry* 21, 2833–2840
- 13 Hoekstra, D. (1982) *Biochim. Biophys. Acta* 692, 171–175
- 14 Bentz, J., Nir, S. and Wilschut, J. (1983) *Colloids Surf.* 6, 333–363.
- 15 Bentz, J., Düzgüneş, N. and Nir, S. (1983) *Biochemistry* 22, 3320–3330
- 16 Wilschut, J., Düzgüneş, N., Hong, K., Hoekstra, D. and Papahadjopoulos, D. (1983) *Biochim. Biophys. Acta* 734, 309–318
- 17 Ohki, S. and Oshima, H. (1984) *Biochim. Biophys. Acta* 776, 177–182
- 18 Ababei, L. and Hildenbrand, K. (1984) *Chem. Phys. Lipids* 35, 39–48
- 19 Silvius, J.R. and Gagné, J. (1984) *Biochemistry* 23, 3232–3240
- 20 Düzgüneş, N., Paiement, J., Freeman, K.B., Lopez, N.G., Wilschut, J. and Papahadjopoulos, D. (1984) *Biochemistry* 23, 3486–3494
- 21 Wilschut, J., Düzgüneş, N., Hoekstra, D. and Papahadjopoulos, D. (1985) *Biochemistry* 24, 8–14
- 22 Bentz, J., Düzgüneş, N. and Nir, S. (1985) *Biochemistry* 24, 1064–1072
- 23 Struck, D.K., Hoekstra, D. and Pagano, R.E. (1981) *Biochemistry* 20, 4093–4099
- 24 Wilschut, J., Nir, S., Scholma, J. and Hoekstra, D. (1985) *Biochemistry* 24, 4630–4636
- 25 Düzgüneş, N., Wilschut, J., Hong, K., Fraley, R., Perry, C., Friend, D.S., James, T.L. and Papahadjopoulos, D. (1983) *Biochim. Biophys. Acta* 732, 289–299.
- 26 Böttcher, C.J.F., Van Gent, C.M. and Fries, C. (1961) *Anal. Chim. Acta* 24, 203–204
- 27 Driessen, A.J.M., Hoekstra, D., Scherphof, G., Kalicharan, R.D. and Wilschut, J. (1985) *J. Biol. Chem.* 260, 10880–10887
- 28 Nir, S., Stegmann, T. and Wilschut, J. (1985) *Biochemistry*, in the press
- 29 Kumar, N., Blumenthal, R., Henkart, M., Weinstein, J.N. and Klausner, R.D. (1982) *J. Biol. Chem.* 257, 15137–15144
- 30 Nichols, J.W. and Pagano, R.E. (1983) *J. Biol. Chem.* 258, 5368–5371
- 31 Ekerdt, R. and Papahadjopoulos, D. (1982) *Proc. Natl. Acad. Sci. USA* 79, 2273–2277
- 32 Rand, R.P. and Parsegian, V.A. (1984) *Can. J. Biochem. Cell Biol.* 62, 752–759